

---

# Physical controls on septic leachate movement in the vadose zone at the hillslope scale, Putnam County, New York, USA

Mark D. Sherlock,<sup>1\*</sup> Jeffrey J. McDonnell,<sup>2</sup> Debra S. Curry<sup>3</sup> and Albert T. Zumbuhl<sup>3</sup>

<sup>1</sup> *Department of Geography, National University of Singapore, 1 Arts Link, Kent Ridge, Singapore 117570*

<sup>2</sup> *Department of Forest Engineering, Oregon State University, Corvallis, Oregon 97331-5706*

<sup>3</sup> *College of Environmental Science and Forestry, State University of New York, Syracuse, NY 13210, USA*

---

## Abstract:

The fate and transport of contaminants in the vicinity of septic fields remains poorly understood in many hydrogeomorphological environments. We report hydrometric data from an intensive hillslope-scale experiment conducted between 29 August and 11 November 1998 at a residential leach field in New York State. The objective of our study was to characterize water flux within the vadose zone, understand the physical controls on the flux, and predict how this ultimately will affect subsurface water quality. Soil-water flux was calculated using matric potential measurements from a network of 25 tensiometer nests, each nest consisting of three tensiometers installed to depths of 10, 50 and 130 cm. Unsaturated hydraulic conductivity curves were derived at each depth from field-determined time-domain reflectometry–tensiometry moisture-release curves and borehole permeametry measurements. Flownets indicated that a strong upward flux of soil water occurred between rainstorms. Following the onset of (typically convective) rainfall, low near-surface matric potentials were rapidly converted to near-saturated and saturated conditions, promoting steep vertical gradients through the near-surface horizons of the hillslope. Lateral hydraulic gradients were typically 10 times smaller than the vertical gradients. Resultant flow vectors showed that the flux was predominantly vertical through the vadose zone, and that the flux response to precipitation was short-lived. The flux response was controlled primarily by the shape of the unsaturated hydraulic conductivity curves, which indicated a rapid loss of conductivity below saturation. Thus, soil water had a very high residence time in the vadose zone. The absence of rapid wetting at 130 cm and the delayed and small phreatic zone response to rainfall indicated that water movement through macropores did not occur on this hillslope. These results are consistent with a Cl tracing experiment, which demonstrated that the tracer was retained in the vadose zone for several months after injection to the system. Copyright © 2002 John Wiley & Sons, Ltd.

KEY WORDS vadose zone; septic leachate; flow pathways

## INTRODUCTION

The fate and transport of subsurface contaminants in many hydrogeological settings remain poorly understood. As human population places increased demands upon surface and groundwater reservoirs for water supply, there is an urgent need to understand the processes controlling the subsurface transport of contaminants. Conventional septic tank and leach-field systems are now used in 24% of USA households for on-site wastewater disposal (Bureau of the Census, 1992). Septic systems are being used in denser population settings around urban fringes, as low-density residential populations expand into suburban zones. In the New York City (NYC) area of the USA, these suburban neighbourhoods are located directly in the water supply catchments for the larger metropolitan area. According to census data from the New York City Department of

---

\*Correspondence to: M. D. Sherlock, Department of Geography, National University of Singapore, 1 Arts Link, Kent Ridge, Singapore 117570. E-mail: geomds@nus.edu.sg

Environmental Protection, about 20 000 conventional septic tank systems are now in use within these water supply catchments. Despite growing public awareness, there are few robust studies on the effects of these septic systems on groundwater and surface water quality at the hillslope and catchment scale.

A typical septic system comprises a septic tank from which clarified effluent flows by gravity to a network of drainage lines, which distribute the effluent into the soil. Although septic tanks may remove a considerable amount of total suspended solids from household wastewater through settling (Canter and Knox, 1985), they have rather limited ability to reduce biochemical oxygen demand (BOD) and total nitrogen (N) owing to the predominant anaerobic conditions (Lawrence, 1973; Canter and Knox, 1985). The receiving vadose zone soils around the distribution lines are relied upon to provide much of the wastewater treatment. However, septic system designs are based primarily upon soil percolation rates and hydraulic loadings, without consideration being given to the effectiveness of the soil in removing pollutants (Huang, 1999). The nitrogen removal capability of these systems is a primary concern for groundwater contamination. In general, septic tank effluents contain large amounts of total Kjeldahl nitrogen (organic nitrogen plus ammonium) and very little nitrate ( $\text{NO}_3^-$ ). Oxidation of organic nitrogen and ammonium ( $\text{NH}_4^+$ ) to  $\text{NO}_3^-$  occurs quickly in the vadose zone beneath the leachlines and causes elevated concentration of  $\text{NO}_3^-$  in groundwater (Wilhelm *et al.*, 1996). Recently, Heisig (2000) has shown that baseflow concentrations of  $\text{NO}_3^-$  and Cl were directly proportional to septic system density in 30 subcatchments of the Croton Watershed, located in the greater metropolitan area of NYC. Elsewhere, Wernick *et al.* (1998) demonstrated the effect of septic system density and location on  $\text{NO}_3^-$  loadings in the Salmon River near Vancouver, Canada. Thus, there is a connection between septic loading and groundwater  $\text{NO}_3^-$  concentrations. Indeed, our work has shown that groundwater wells up to 30 m down-gradient of leachate distribution lines show elevated  $\text{NO}_3^-$  levels at various times of the year in the Croton watershed, several times in excess of the U.S. Environmental Protection Agency drinking water quality standard (Curry, 1999).

The efficiency and functionality of septic systems is highly dependent on site-specific factors such as soil physical properties and soil-water energy distributions (Amoozegar, 1997). Although several studies in the NYC area (Curry, 1999) and elsewhere (Harman *et al.*, 1996) have shown how migration of leachate-rich water occurs in the phreatic zone, the controls on water and leachate movement in the vadose zone in, around and downslope from leachfields is not well described. In North Carolina, Penninger and Hoover (1998) provided hydrometric evidence that downslope effluent flow occurred from a septic system through the upper soil horizons of a clayey soil, as a result of perched saturation over an impeding B/C horizon. Although this flow pathway potentially provides the opportunity for extended aerobic treatment of effluent, the magnitude of the flux was not specified. Further, restricted vertical percolation in a septic leachfield increases the risk of surface effluent ponding, and thus, system failure (Wolf *et al.*, 1998). Overland flow may then transport untreated effluent directly to sensitive zones such as reservoirs or poorly sealed drinking water wells. Other studies of septic effluent migration have observed rapid vertical percolation of effluent through highly permeable (e.g. Robertson *et al.*, 1991) and/or macroporous (e.g. Brown *et al.*, 1979; McKay *et al.*, 1993) subsoils. Where effluent migration is vertical and rapid beneath leach lines, the potential for groundwater contamination is elevated because of the short residence time of effluent (and thus limited opportunity for treatment) in the vadose zone. Conversely, soils with high saturated hydraulic conductivities, such as sands, tend to have very steep moisture-release curves and rapidly lose permeability below saturation. Where these soils are unsaturated, water and effluent is immobilized and retained within the vadose zone, increasing effluent exposure to aerobic treatment processes (e.g. Cogger *et al.*, 1988). Anderson *et al.* (1994) demonstrated that considerable treatment of septic tank effluent occurred in the vadose zone of a fine sandy soil in Florida, and that this was directly attributable to the steep moisture-release curve of this soil. Similar data for glaciated regions with podzolized soil are rare. In the context of the NYC water supply no data exist on how soils developed in glacial till might control vadose zone movement of septic leachate.

This paper is part of a larger study investigating the fate and transport of septic effluent in the NYC water supply catchments (Curry, 1999). In this paper, we explore the physical controls on soil water movement in the vadose zone of a residential septic field in Putnam County, NY. Previous Cl water tracing experiments

at this site indicated that much of the tracer mass was retained within the vadose zone in the vicinity of the septic distribution lines. To explain the flow mechanisms controlling soil-water movement in the septic field, we present hydrometric data collected along a topographic flow line extending 30 m downslope from the septic distribution lines. The data were collected between September and mid-November 1998, when the soil moisture deficit was very high following a relatively dry summer. We examine hillslope-scale vadose zone flux of water as an ultimate control on leachate migration within the phreatic zone. Our objectives are:

1. to determine the magnitude and direction of soil water flux in the vadose zone of a residential septic field;
2. to examine the physical controls on the flux characteristics during and among rainstorms;
3. to explore linkages between vadose zone flux and observed tracer distributions in the phreatic zone.

### SITE DESCRIPTION

A 50 by 50 m plot was established in and around a residential septic field in the township of Patterson, Putnam County, south-eastern New York (Figure 1). The field site lies within the Croton watershed, which provides approximately 10% of the NYC water supply. The septic system is gravity-fed and comprises a 3785 L septic tank from which effluent flows to a distribution box. The distribution box channels the effluent through three 34-m parallel distribution lines, which distribute the effluent into the unsaturated soil matrix. The septic system serves a three-bedroom house, in which two people reside. Daily effluent flow is estimated at 2271 L per day.

The soils are Charlton loams (a coarse-loamy, mixed, mesic Typic Dystrochrept), which formed from a stratified glacial drift deposit. The soil profile typically comprises a sandy loam  $A_p$  horizon (0–20 cm), a loam B horizon (20–80 cm), and a silt loam C horizon (>80 cm). Visible root channels are fine and confined to the upper 40 cm of the profile. These channels are abundant within the upper  $A_p$  horizon at 0–5 cm depth. The field is abandoned pasture land, with shallow slopes ranging from 2° to 8°. Rainfall averages 1160 mm annually.

### METHODOLOGICAL APPROACH

An intensive hydrological investigation was conducted at the study site between 29 August and 13 November 1998. This period represents a time of significant groundwater recharge, during which the water table elevation below the septic distribution lines rose by more than 1 m. Hydrometric, water tracing and geophysical techniques were used during investigation at the site. The hydrometric data set comprises tensiometric and piezometric measurements, which were combined with measurements of soil physical properties to characterize water flux within the hillslope. In this paper, we focus on the hydrometric measurements taken from the vadose zone of the hillslope, although reference is made to soil-density profiles obtained from the use of a dynamic cone penetrometer, the results of a Cl water-tracing experiment, the phreatic-zone piezometric response and groundwater chemistry.

Matric potential ( $h$ ) was monitored using a network of 25 tensiometer nests distributed across the septic field. A topographic flow line extending downslope of the leach lines was instrumented with 13 of the tensiometer nests, spaced at 2.5 m intervals down the slope. Each nest comprised three tensiometers installed to depths of 10, 50 and 130 cm, which are coincident with the  $A_p$ , B and C horizons of the soil profile. Matric potential was measured manually using a Soil Measurement Systems 'Tensimeter'. The sampling resolution was daily between rainstorms and increased to hourly during and following rainstorms when vadose zone response was potentially more dynamic. Matric potential was monitored intensively over five rainstorms during the experimental period. These rainstorms ranged in magnitude from 8 mm to 70 mm. Peak rainfall intensities and antecedent soil wetness conditions varied among the rainstorms (Figure 2).

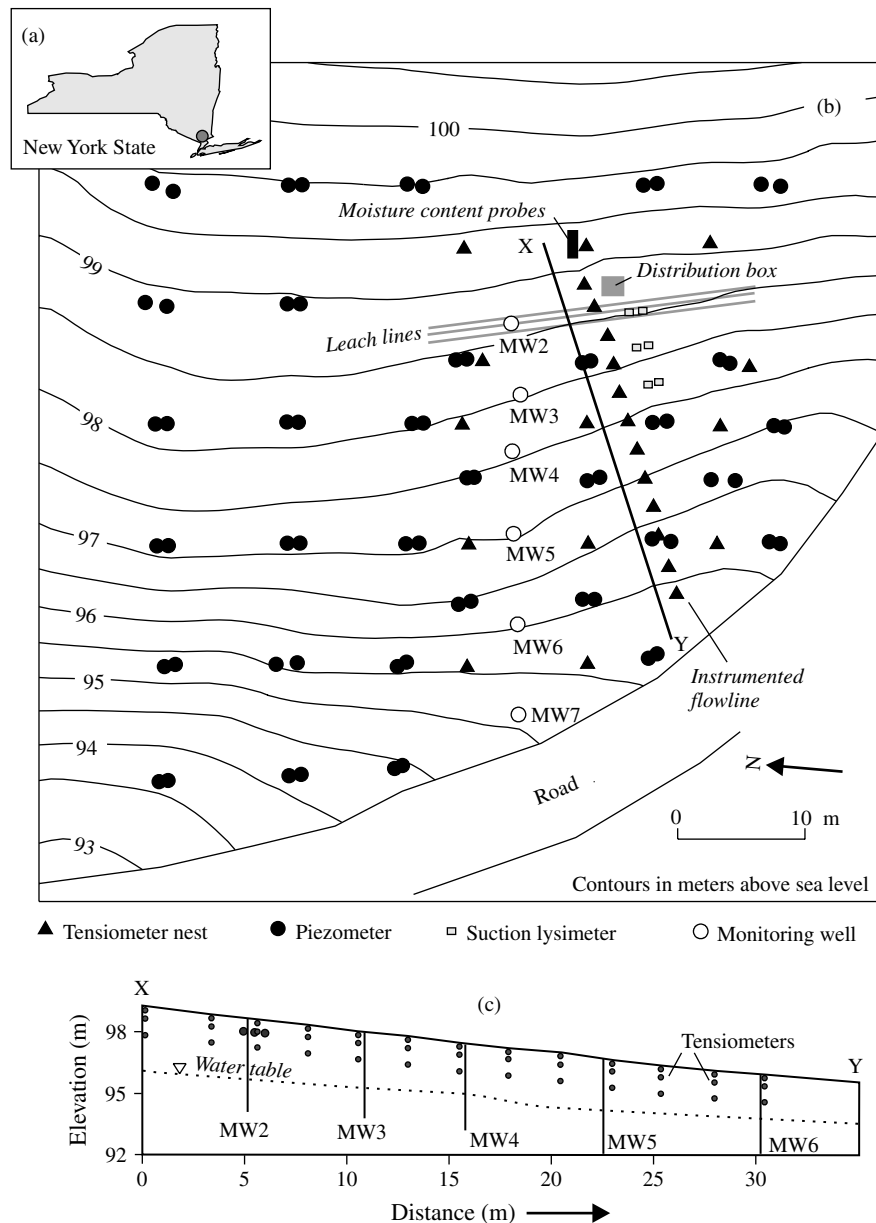


Figure 1. (a) Regional field site location. (b) Field site instrumentation layout. (c) Cross-section along instrumented flowline

The saturated hydraulic conductivity ( $K_{\text{sat}}$ ) of the vadose zone was determined from 43 borehole permeametry measurements (Amoozegar, 1997). Moisture release curves (i.e. the relationship between volumetric moisture content ( $\theta$ ) and ( $h$ )) were determined at 10, 50 and 130 cm using three Campbell Scientific soil-moisture reflectometers co-located with the upslope tensiometer array (Figure 1). These curves were derived empirically from measurements of porosity and particle-size distribution (Van Genuchten, 1980; Rawls and Brakensiek, 1989). The unsaturated hydraulic conductivity curve,  $K(h)$ , at 10, 50 and 130 cm soil depths was obtained using methods described by Millington and Quirk (1960). The matric potential measurements were

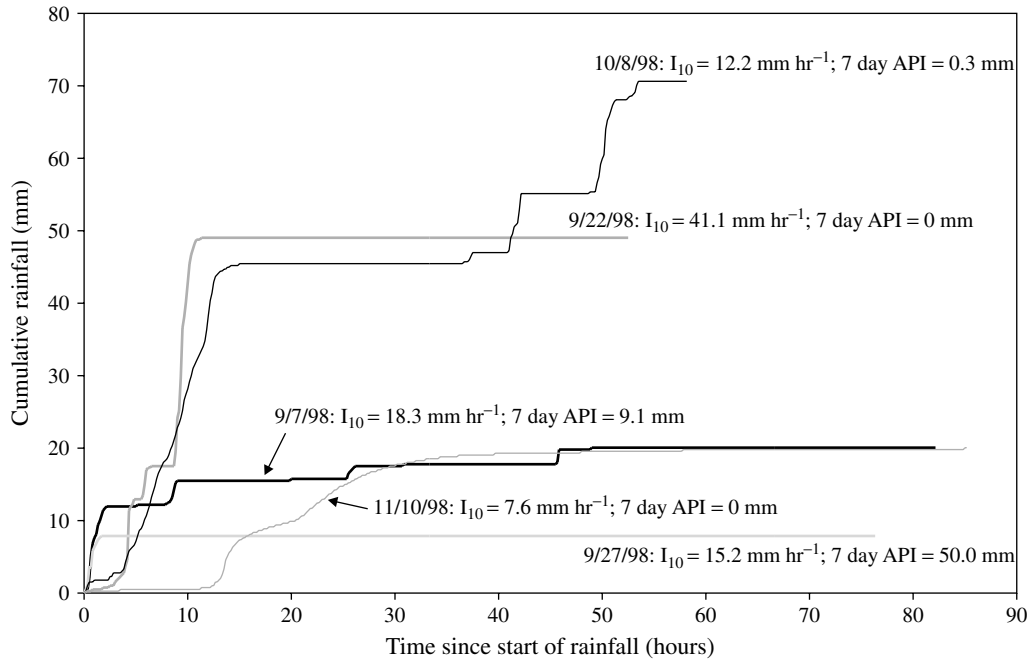


Figure 2. Rainfall characteristics of the five rainstorms, where  $I_{10}$  is the peak 10-min rainfall intensity and 7 day API is the unweighted 7-day antecedent precipitation index

used to estimate the hydraulic conductivity from the  $K(h)$  curves for each measurement time-step at each tensiometer locality.

Macroscopic water flux ( $q$ ) within the vadose zone was quantified using the steady-state form of the Darcy–Buckingham equation (Darcy, 1856; Buckingham, 1907)

$$q = K(h) \times \frac{d(H)}{L} \quad (1)$$

where  $K(h)$  is the hydraulic conductivity as a function of matric potential ( $h$ ) and  $d(H)/L$  is the hydraulic gradient, with  $H$  the sum of  $h$  and elevation potential,  $z$ , and  $L$  the linear distance over which the hydraulic gradient is measured. Both lateral (downslope) and vertical flux calculations were performed using the  $K(h)$  and  $d(H)/L$  data, and these fluxes were resolved using equations presented by Harr (1977)

$$qR = \sqrt{(qD + qV \times \sin \alpha)^2 + (qV \times \cos \alpha)^2} \quad (2)$$

$$\gamma = \sin^{-1}(qD \cdot \cos \alpha / qR) \quad (3)$$

where  $qR$ ,  $qD$  and  $qV$  are the resultant, downslope and vertical macroscopic fluxes, respectively;  $\alpha$  is the slope angle; and  $\gamma$  is the angle of the resultant flux ( $0^\circ$  is vertically downwards and  $90^\circ$  is horizontally downslope). The accuracy of the resultant angle of flow is dependent upon the assumption that the soil is anisotropic.

A network of 32 piezometer nests was installed into the phreatic zone in and around the leachfield (Figure 1). Each nest comprised both a shallow and a deep piezometer for the calculation of hydraulic gradients in the vertical plane. For each nest, the vertical separation of the screening between the shallow and deep piezometers was typically around 1 m. The distributed nested approach also enabled lateral hydraulic gradient calculations.

## RESULTS AND DISCUSSION

*Soil physical properties*

The permeametry data set indicated that  $K_{\text{sat}}$  decreased with depth through the soil profile (Figure 3). Geometric means of  $K_{\text{sat}}$  in the  $A_p$ , B and C horizons respectively were 4.1, 5.5 and 0.66  $\text{cm h}^{-1}$ . This decrease was associated with increasing overburden compression, a reduction in fine roots and an increase in silt with depth. Forty piezometer recovery tests indicated that  $K_{\text{sat}}$  within the phreatic zone was highly variable across the septic field, although the geometric means of the shallow and deep piezometer  $K_{\text{sat}}$  data were similar (0.11  $\text{cm h}^{-1}$  and 0.17  $\text{cm h}^{-1}$ , respectively). Therefore, no significant hydraulic discontinuity was evident between the unsaturated C horizon and the phreatic zone.

A comparison of field-measured  $K_{\text{sat}}$  with short-term rainfall intensities gives some indication of the direction of water and effluent flux through the unsaturated soil profile (Figures 2 and 3). Peak 10-min rainfall intensities were much lower than near-surface  $K_{\text{sat}}$  over the five monitored rainstorms. Therefore, significant downslope deflection of soil water and effluent within the B and C horizons ordinarily would not be expected. During the 22 September 1998 rainstorm, however, short-term intensities approached the near-surface  $K_{\text{sat}}$ . Given the marked increase in root density within the upper 5 cm of the profile, actual surface infiltration rates are probably much greater than the near-surface  $K_{\text{sat}}$ . Surface ponding and infiltration-excess overland flow were not observed on the hillslope during the experimental period. Between the  $B_1$  and C horizons,  $K_{\text{sat}}$  values decreased by approximately one order of magnitude. The  $K_{\text{sat}}$  values within the C horizon were generally lower than peak short-term rainfall intensities measured during the rainstorms. Vertical percolation of soil water through the C horizon may become impeded if high rainfall intensities prevail following wetting of the overlying horizons. Under these circumstances, the soil-water and effluent-flow vectors must comprise a downslope flow component within the C horizon. Rainfall intensities exceeding the C horizon  $K_{\text{sat}}$  were short-lived (up to 10 min duration), suggesting that flux during and among rainstorms was predominantly vertical at this depth within the septic field.

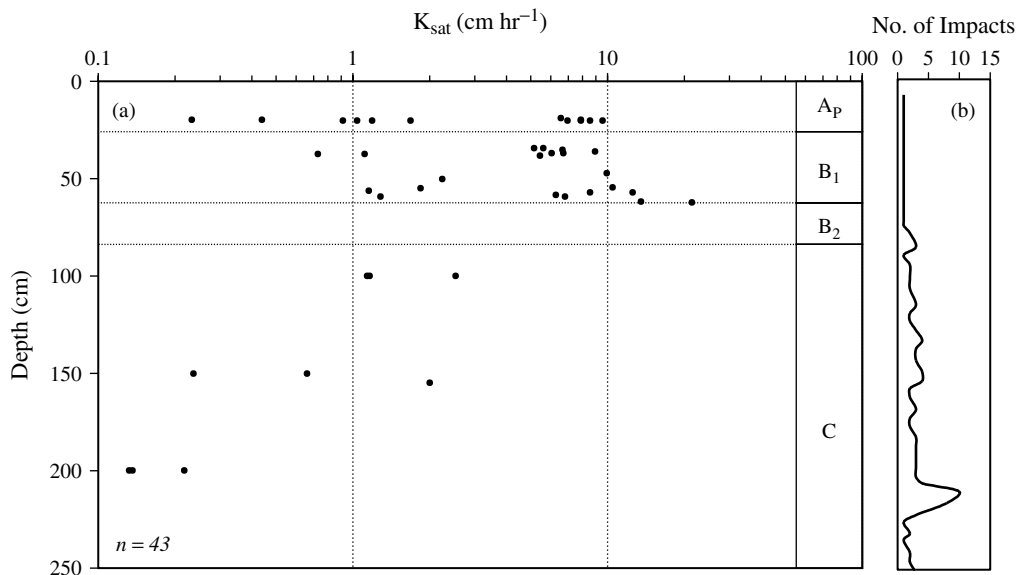


Figure 3. (a) Vadose zone saturated hydraulic conductivity determined from borehole permeametry, and (b) a typical soil strength/density profile determined using a dynamic cone penetrometer. Number of impacts is the hit count required to drive the cone through 5 cm of soil

The field-measured  $\theta(h)$  curves at 10, 50 and 130 cm are shown in Figure 4. The predicted  $\theta(h)$  curves derived from the Rawls and Brakensiek (1989) technique are overlain, but matched poorly against the field-determined  $\theta(h)$  curves. With decreasing  $h$  at 10 cm, the predicted decrease in  $\theta$  was much greater than the measured decrease in  $\theta$ . Conversely, at 130 cm the predicted loss of  $\theta$  with decreasing  $h$  was smaller than was actually measured. Thus, there was no consistency between the measured and modelled curves, indicating that the uncertainties associated with the predictive approach can be significant. Therefore, field-derived  $\theta(h)$  curves are used in the subsequent discussion. Volumetric moisture content at saturation was greatest at 10 cm, and smallest at 130 cm, which indicates that total porosity decreased with depth in the soil profile. This is consistent with the measured vertical  $K_{\text{sat}}$  distributions in the vadose zone. Near saturation, the  $A_p$  horizon at 10 cm depth exhibited the greatest decrease in moisture content with decreasing  $h$ . However, the loss of moisture content within this matric potential range was smaller at 50 cm and 130 cm, suggesting that changes in hydraulic conductivity below the  $A_p$  horizon were less dynamic during rainstorms. A Millington and Quirk (1960) type analysis of the moisture release curves indicated that the magnitude of hydraulic conductivity was highly sensitive to matric potential changes in the  $A_p$ , B and C horizons. From 0 to  $-10$  cm  $H_2O$   $h$ , hydraulic conductivity decreased by almost three orders of magnitude in those horizons (Figure 5). Therefore, when antecedent soil moisture is high, water flux is highly responsive to increases in  $h$  associated with rainfall inputs through the soil profile.

#### Soil water variables: temporal distributions

Data from the 39 tensiometers installed along the topographic flowline (Figure 1) indicated that  $h$  at any given time was highly dependent upon measurement depth and exhibited little variability downslope at that depth. In the  $B_1$  and C horizons,  $h$  typically varied by less than 50 cm  $H_2O$  within each horizon along the flowline at a given time, indicating that the water content in the deeper horizons is relatively uniform across the hillslope. However, within the  $A_p$  horizon, the  $h$  range along the flowline increased markedly during periods of no rainfall (e.g. between the 7 September and 22 September 1998 storms). Presumably, this resulted from two

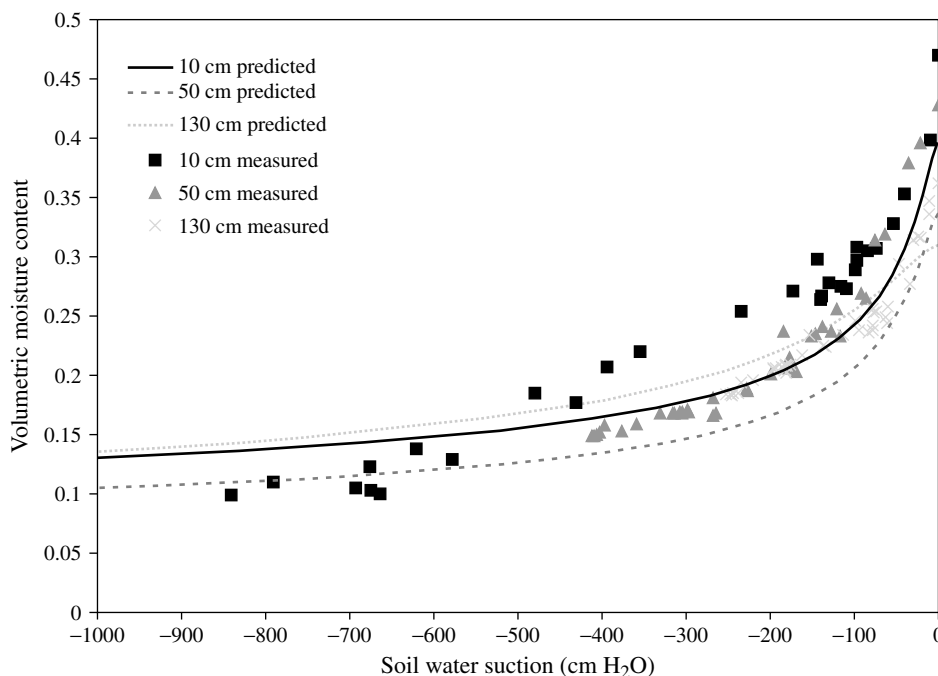


Figure 4. Field-measured and predicted moisture release curves at 10, 50 and 130 cm depths in the septic field

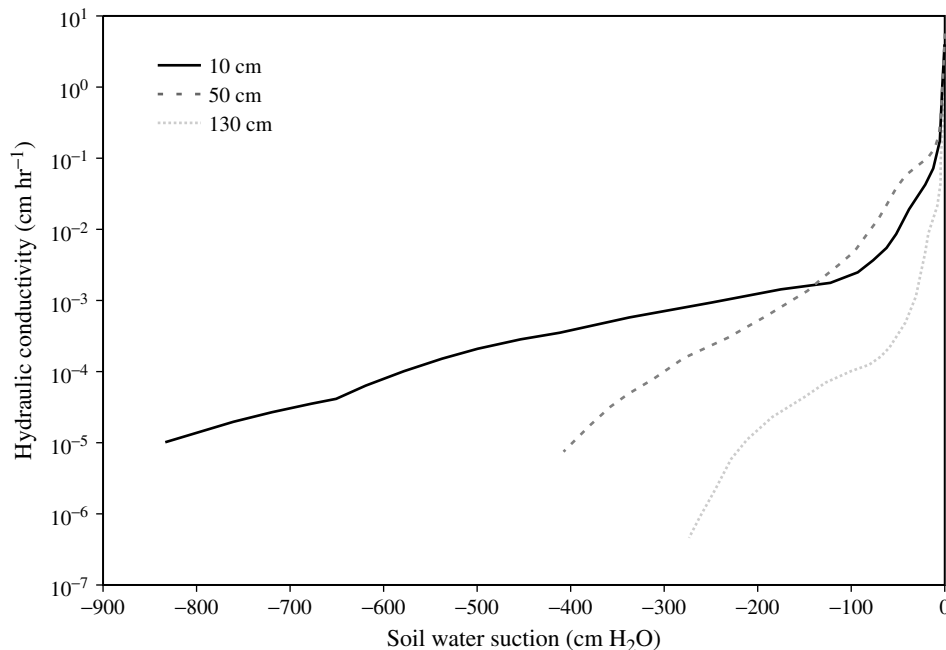


Figure 5. Unsaturated hydraulic conductivity curves derived using the Millington and Quirk (1960) method on the field-measured moisture release curves

key factors. Firstly, tall deciduous trees, which line the south-western perimeter of the study site, shaded much of the lower slope elevations during the afternoon hours, and resulted in highly variable solar radiation inputs to the soil surface along the instrumented flowline. Therefore, during dry periods, evapotranspiration was probably greater at the top of the slope, causing greater decreases in  $h$ . Secondly, permeability measurements indicated that  $K_{\text{sat}}$  ranged by over 1.6 orders of magnitude in the  $A_p$  horizon (Figure 3), probably because of textural variability across the hillslope. Such variability would lead to variable moisture losses within this horizon from both drainage and evapotranspiration.

During rainfall,  $h$  variability within the  $A_p$  horizon was rapidly reduced, as saturation was typically achieved within this horizon across the hillslope within minutes of the onset of intense rainfall. Saturation was attained at the 10 cm depth in the  $A_p$  horizon during four of the five monitored rainstorms (Figure 6).

The frequency of saturation within the  $A_p$  horizon was unexpected, given the near-surface  $K_{\text{sat}}$  measurements and peak rainfall intensities discussed above. In the light of previous studies (e.g. Wilson *et al.*, 1989; Sherlock *et al.*, 2000) it is unlikely that the borehole permeametry technique overestimated the effective  $K_{\text{sat}}$  of the hillslope soils. Saturation within the  $A_p$  horizon may have been induced by a short-term hydraulic discontinuity within the  $B_1$  horizon, which existed because this horizon remained unsaturated even over intense rainstorms (Figure 6). The  $B_1$  horizon  $K(h)$  curve demonstrates that the field-state hydraulic conductivity was typically two to three orders of magnitude below measured  $K_{\text{sat}}$  (Figures 3 and 5). Although vertical hydraulic gradients typically approached 6 when the  $A_p$  horizon attained saturation (Figure 7), this is not sufficient to compensate for the decreased field-state hydraulic conductivity of the  $B_1$  horizon. This leads to the development of perched saturation within the  $A_p$  horizon, as rainfall inputs to the soil surface exceed the vertical flux rate to the  $B_1$  horizon.

Flow impedance to the  $B_1$  horizon is further evidenced by the delayed wetting front arrival times. Significant changes in  $h$  in the  $B_1$  horizon were observable 5 h after the beginning of the 22 September 1998 rainstorm, 8 h after the beginning of the 8 October 1998 and 10 November 1998 rainstorms and 1 day after the beginning

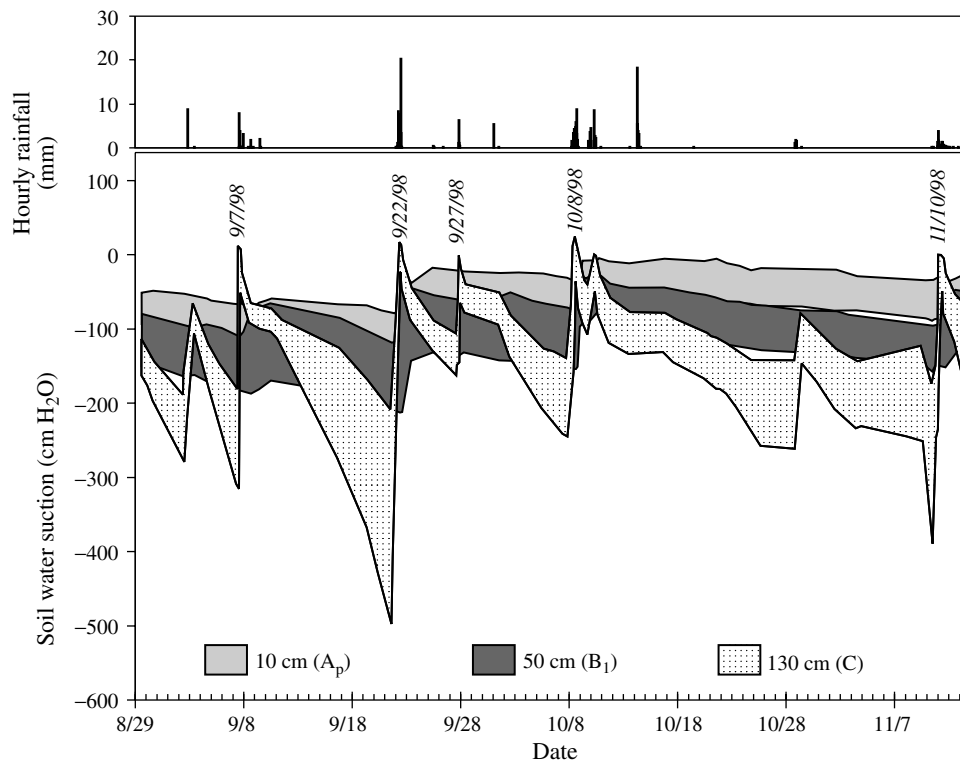


Figure 6. Matric potential ranges within the  $A_p$ ,  $B_1$  and C horizons along the instrumented flowline. Each horizon-specific suction range is derived from 13 time-series data sets

of the 7 September 1998 rainstorm. No significant wetting of the  $B_1$  horizon was observed during the 27 September 1998 storm, presumably because of the small magnitude of the rainstorm. The timing of wetting within the C horizon was similar to that within the  $B_1$  horizon, or lagged only slightly behind. This suggests that, despite the  $K_{sat}$  discontinuity (Figure 3), flow between these horizons is not impeded. This is consistent with cone penetrometer data collected across the site, which consistently indicated that the penetrability was relatively constant between the  $B_1$  and C horizons (Figure 3).

The dynamic response of the  $A_p$  horizon to rainfall (Figure 6) resulted in rapid and marked changes in the magnitude of the hydraulic gradients between the  $A_p$  and  $B_1$  horizons (Figure 7). Prior to rainfall, these gradients were often negative and large (exceeding  $-6$  cm prior to the 22 September 1998 rainstorm), indicating a strong upwards flux of soil moisture required to replace evapotranspirative losses. Following the onset of rainfall, the negative vertical gradients were rapidly reversed and converted to large positive gradients, indicating vertical flow towards the  $B_1$  horizon. Vertical gradients between the  $B_1$  and C horizons were almost always positive, typically ranging between 0 and 0.5 between rainstorms and increasing to 0.5–1 following rainfall. The gradients at this depth were much less dynamic than those between the A and  $B_1$  horizons, which is consistent with the  $h$  responses.

The lateral hydraulic gradients were much smaller than the vertical hydraulic gradients (Figure 7). Although vertical gradients between the  $A_p$  and  $B_1$  horizons were between 2 and 4 following rainfall, lateral gradients through the  $A_p$  horizon never exceeded 0.8. The lateral gradients were generally positive, indicating that this flow component, although small, was in the downslope direction. Lateral gradients at 50 cm and 130 cm depths were small, generally between 0 and 0.2. Again, this indicates a very small lateral flow component at these depths.

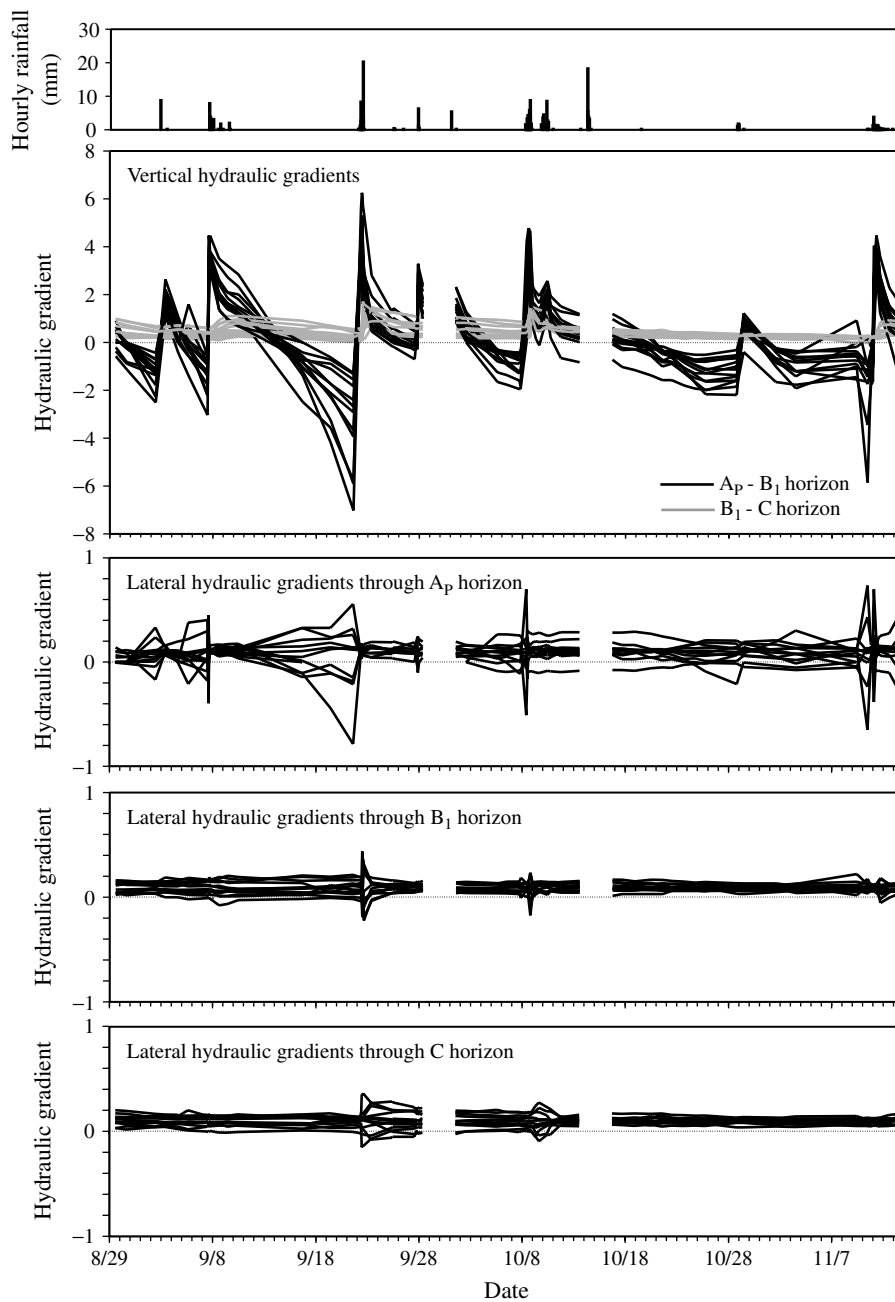


Figure 7. Measured vertical and lateral hydraulic gradients along the instrumented flowline

#### *Soil-water variables: spatial distributions*

The distribution of total potential along the instrumented flowline was examined in the vadose zone during individual rainstorms. This enabled a two-dimensional spatial visualization of the direction and magnitude of the hydraulic gradients. These data were coupled with piezometric head data measured in the phreatic zone along the instrumented flowline to examine hydrological linkages between the vadose and phreatic zones,

and the implications for effluent transport. Figure 8 illustrates the time-series of both (a) matric potential and piezometric head, and (b) total potential distribution along the instrumented flowline at each monitored time-step over the 8 October 1998 rainstorm. The vertical bars on the hyetograph indicate the time of matric potential measurement.

Elevated moisture contents directly below or downslope of the septic distribution lines were not apparent from the tensiometric data (Figure 8; time  $t_1$ ). This indicates that either the effluent discharge to the soil across the distribution lines was small, and/or the effluent was not being discharged into the soils in the vicinity of the instrumented flowline. The near-surface upward flux of water prior to rainfall is illustrated in Figure 8 (time  $t_1$ ). This flow was rapidly reversed following the onset of rainfall as the  $A_p$  horizon rapidly approached saturation (Figure 8; time  $t_2$ ). With continued wetting of the  $A_p$  horizon, the hydraulic gradients between the  $A_p$  and  $B_1$  horizons steepened (Figure 8; times  $t_3$  and  $t_4$ ). These gradients decreased slowly following the cessation of rainfall as the  $A_p$  horizon drained and the wetting front progressed through the  $B_1$  horizon (Figure 8; times  $t_5$  and  $t_6$ ). The form of the equipotentials between the  $B_1$  and C horizons changed only slightly during the rainstorm. Further, the water table and piezometric head response to the rainstorm was negligible.

#### *Resultant soil-water flow vectors*

The lateral and vertical water-flux components are summarized in Table I for the 8 October 1998 rainstorm. The extent of anisotropy in the soils was not determined. However, if the Harr (1977) approach is used to determine flux direction in soils exhibiting marked anisotropy (i.e. having a much greater lateral hydraulic conductivity relative to vertical hydraulic conductivity), and if the experimental approach did not explicitly determine the extent of anisotropy, then the significance of the lateral flow pathway could be underestimated. However, vertical flux typically exceeded lateral flux by over one order of magnitude (Table I), and given the shallow slope angle, the effect of anisotropic soils on the flow direction resolved using the Harr (1977) approach, should be small.

Figure 9 illustrates the calculated resultant flow vectors between the  $A_p$  and  $B_1$  horizons, and the  $B_1$  and C horizons down the hillslope over the 8 October 1988 rainstorm. Prior to rainfall (Figure 9; time  $t_1$ ), water flux between the A and  $B_1$  horizons ranged between  $10^{-3}$  and  $10^{-2}$  cm hr $^{-1}$  and was predominantly vertical. Flux magnitudes between the  $B_1$  and C horizons were generally one order of magnitude lower, and exhibited slight lateral downslope components. This reflects the reduced field-state hydraulic conductivity below the  $B_1$  horizon. During the initial stages of rainfall (Figure 9; times  $t_2$  and  $t_3$ ), flow vectors between the  $A_p$  and  $B_1$  horizons were highly variable in magnitude and direction, because of localized wetting front arrival in the  $A_p$  horizon. At time  $t_4$ , the  $A_p$  horizon was near-saturated or saturated along the length of the flowline (Figure 8), following the delivery of approximately 30 mm rainfall. This resulted in vertical soil-water flux rates of approximately 10 cm h $^{-1}$  across the hillslope, whereas the flow vectors between the  $B_1$  and C horizons remained unchanged. Soil-water flux between the  $A_p$  and  $B_1$  horizons declined rapidly following the cessation of rainfall at time  $t_6$ , and was paralleled by an increase in flux between the  $B_1$  and C horizons as the wetting front propagated through the profile. Flux between these horizons generally increased by one order of magnitude at time  $t_6$ , ranging between  $10^{-3}$  to  $10^{-1}$  cm h $^{-1}$ . As the  $B_1$  and C horizons drained (times  $t_7$  and  $t_8$ ), initially at the head of the hillslope (Figure 8), the loss of hydraulic conductivity resulted in the flux approaching the pre-storm magnitudes. Throughout the rainstorm, resultant flow vectors exhibited a predominant vertical direction through the  $B_1$  and C horizons.

With the exception of the 27 September 1998 rainstorm, the flow vectors exhibited over the 8 October 1998 rainstorm event were characteristic of the flux responses observed over the other monitored rainstorms. Flux response to the 27 September 1998 rainstorm was negligible because the rainfall was insufficient for significant soil wetting.

The residence time of effluent was estimated, based on the hydrometric data and the following assumptions:

1. effluent movement is vertical and flows at the same rate as the soil water (i.e. by advective transport);

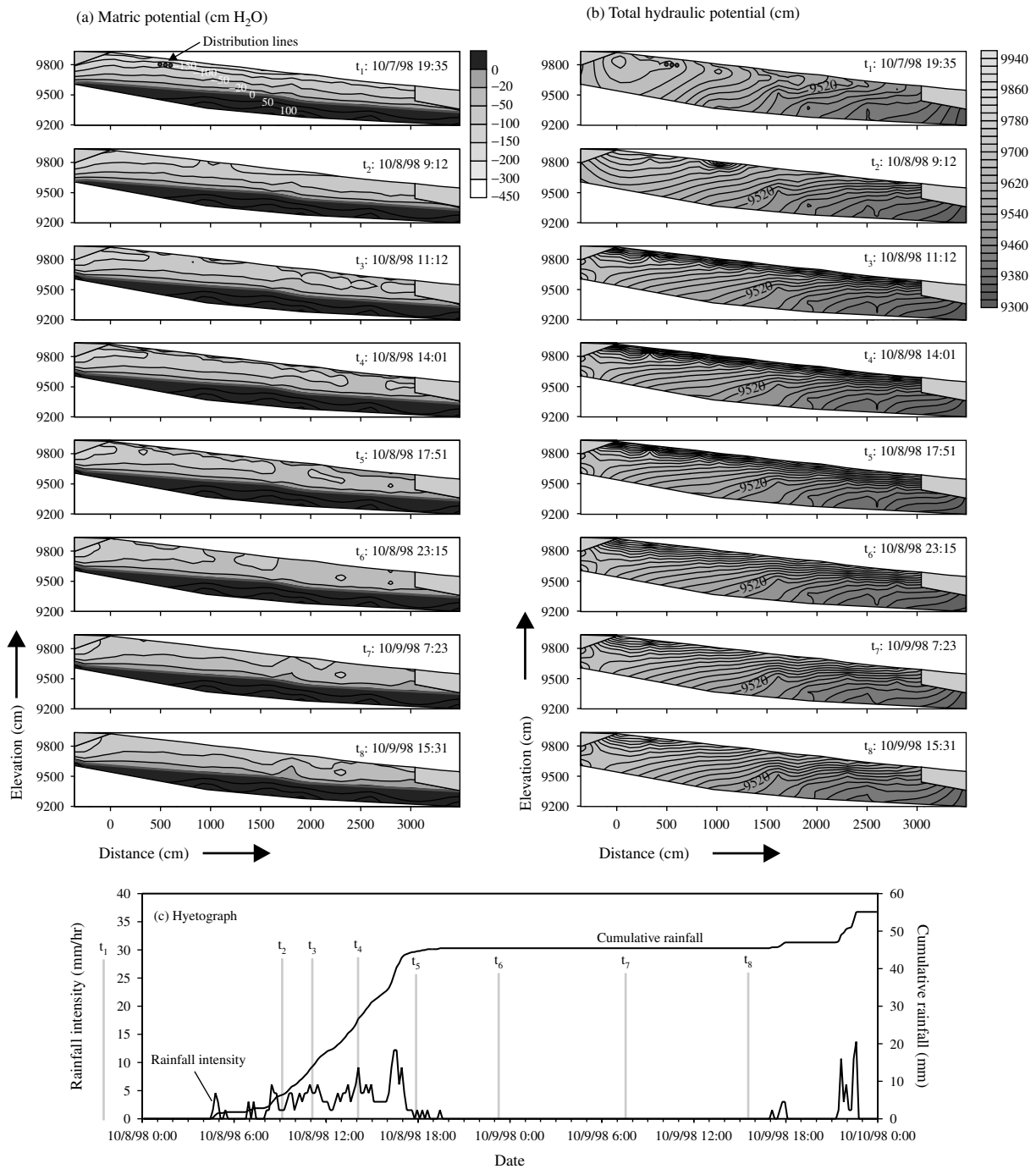


Figure 8. (a) Matric potential and (b) total potential distributions along the instrumented flowline, and (c) rainfall over the 8 October 1998 rainstorm

Table I. Summary of calculated lateral and vertical flux magnitudes prior to and at the peak of the rainfall event on 8 October 1998

Direction of Flux	Distance depth	Pre-storm flux		Flux at peak of storm (at time t <sub>5</sub> : 1751 hours)	
		Mean flux (cm h <sup>-1</sup> )	Flux range (cm h <sup>-1</sup> )	Mean flux (cm h <sup>-1</sup> )	Flux range (cm h <sup>-1</sup> )
Lateral	10 cm	1.0E-4	1.0E-5 to 4.0E-4	4.0E-1	1.0E-1 to 1.0E0
	50 cm	5.0E-4	3.0E-5 to 2.0E-3	4.0E-3	1.0E-4 to 1.0E-2
	130 cm	3.0E-5	3.0E-7 to 1.0E-4	3.0E-5	2.0E-7 to 1.0E-4
Vertical	10–50 cm	3.0E-3	9.0E-4 to 6.0E-3	4.0E0	2.0E-1 to 8.0E0
	50–130 cm	2.0E-3	2.0E-4 to 6.0E-3	2.0E-2	2.0E-4 to 8.0E-2

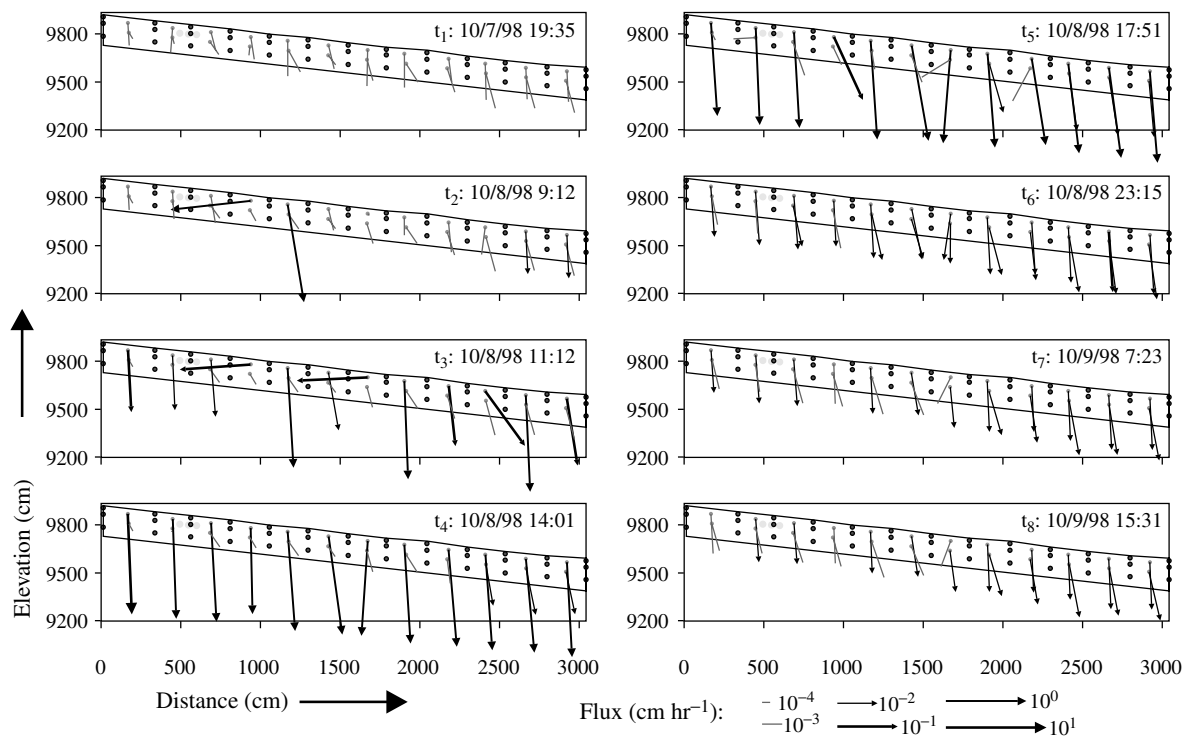


Figure 9. Magnitude and direction of water flux in the vadose zone over the 8 October 1998 rainstorm. Flow vectors are calculated using the approach of Harr (1977)

2. there is a 2 m vertical separation distance between the distribution lines and the water table;
3. the effective porosity of the B<sub>1</sub> and C horizons averages 25%.

Based on the data collected between 29 August and 13 November 1998, the travel time of the septic effluent through the vadose zone of the hillslope ranged from 200–500 days (according to calculations developed by Sherlock *et al.* (2000)).

#### Flow pathway evidence from Cl tracing

A Cl tracing experiment was conducted on 7 October 1998, and is described in detail in Curry (1999). The objective of this work was to make direct observations of flow direction and magnitude through the vadose and

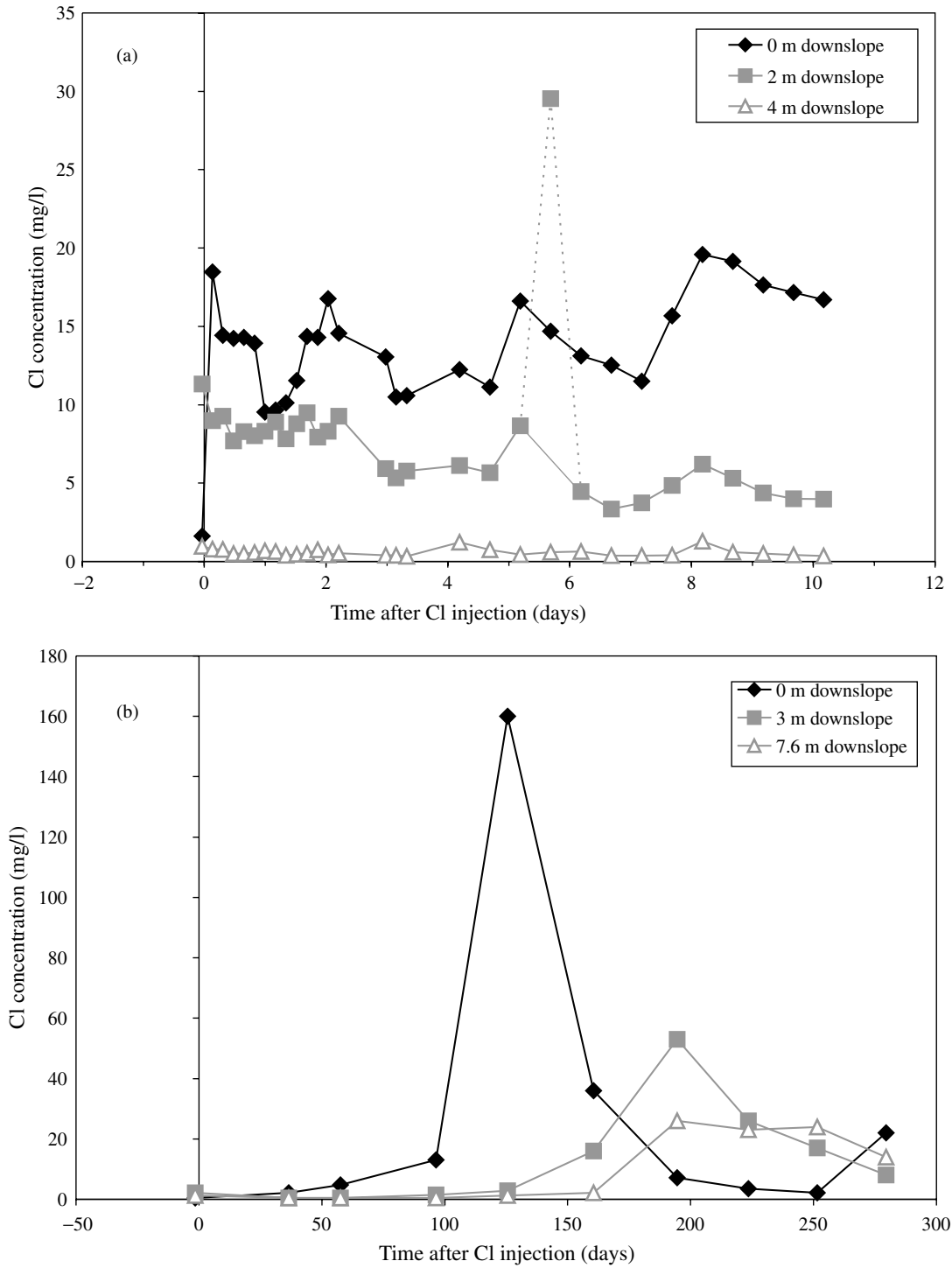


Figure 10. Concentrations of Cl in (a) the vadose zone at 100 cm depth, and (b) in the phreatic zone

phreatic zones of the hillslope. The Cl tracing experiment results are used here for comparison with the flow pathways indicated by the hydrometric investigation. Figure 10 illustrates that some of the Cl tracer (injected into the septic junction box) migrated vertically to 100 cm depth (40 cm below the leach lines) within 6 h of injection, where it remained for the following 10 days. Measured Cl concentrations at this locality were more than three orders of magnitude lower than input Cl concentrations to the distribution box. Presumably significant mixing of the Cl tracer occurred with effluent from the septic tank in both the distribution system and the vadose zone soils. No downslope migration of the tracer was observed in the vadose zone over the first 10 days following Cl injection. Unfortunately Cl monitoring in the vadose zone ceased after day 10 of the experiment, because the onset of overnight freezing would have damaged the automatic sampler. Breakthrough of Cl in the phreatic zone was delayed. Tracer concentrations in the groundwater vertically below the leachlines (MW2; see Figure 1) peaked 125 days after injection (10b). Concentrations of Cl in groundwater 3 m downslope of the leachlines (MW3) peaked almost 200 days after injection.

These results are consistent with our hypothesis that effluent movement within the vadose zone is both vertical and slow during this time of the year. Piezometric data indicated small and delayed increases in head 1–3 days after rainstorms (Figure 11), which presumably resulted from the downward displacement of pre-event water stored within the lower C horizon of the vadose zone.

### CONCLUSIONS AND IMPLICATIONS

Septic system efficiency is often related to many site-specific soil physical properties. Whereas most studies to date have documented this in relation to phreatic zone processes, this study focused on the physical controls on septic leachate movement in the vadose zone. Data from this study suggest that water and leachate flux in the vadose zone in, around and downslope from the leachfields is controlled by a number of physical factors (some distinct from those controls on the saturated flux). The shape of moisture-release curves, and the resulting hydraulic conductivity functions resulted in a rapid loss of hydraulic conductivity with matrix drainage in the  $A_p$ ,  $B_1$  and C horizons. Field state hydraulic conductivity typically decreased with depth, because of both the

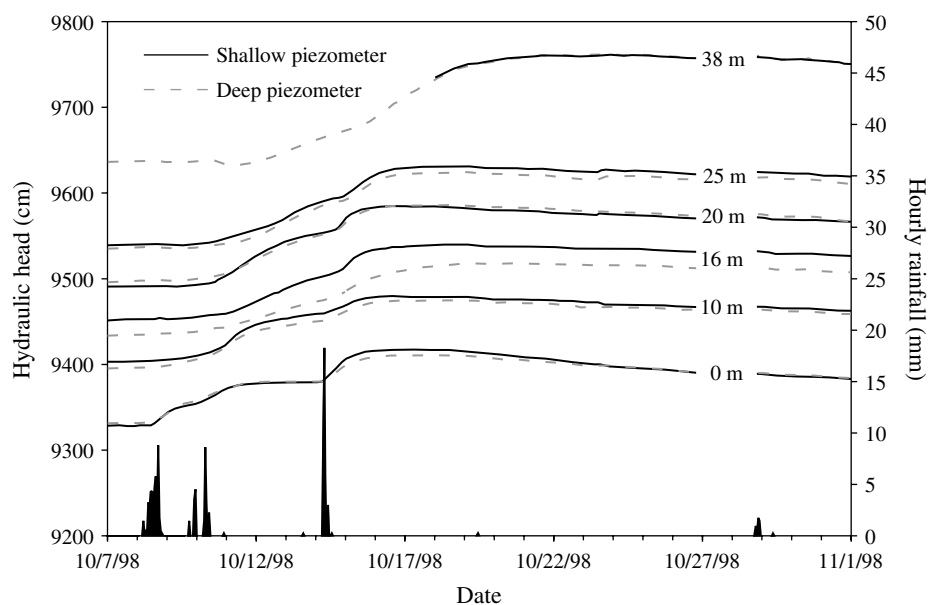


Figure 11. Piezometer response following the 8 October 1998 rainstorm. Distances indicate distance upslope from the foot of the hillslope

reduction in  $K_{\text{sat}}$  with depth, and the limited wetting of the B<sub>1</sub> and C horizons during rainstorms. Secondly, the vertical hydraulic gradients were much steeper than the lateral gradients, because of both the shallow slope angle and the pronounced wetting, which typically occurred in the near-surface. Thirdly, visible macropore space was confined to the very near-surface, above the depth of the buried leach lines. Thus, soil water and effluent migration probably occurs within matrix pore-space, and therefore is controlled by the key elements in soil-water physics; field-state hydraulic conductivity and hydraulic gradients.

We demonstrated that flux within the vadose zone was predominantly vertical, and dynamic during five rainstorms occurring between 29 August and 13 November 1998. However, the response to rainfall was typically short-lived (of the order of a few hours), and the calculated peak fluxes between the B<sub>1</sub> and C horizons were relatively small. Our calculations indicated that septic effluent has a long residence time of between 200 and 500 days within the vadose zone during this time of the year.

These findings are broadly consistent with the results of a Cl tracer experiment, which suggested that the tracer mass was retained within the matrix pore space directly below the distribution lines for several months after Cl injection (Curry, 1999). Thus, the predominantly vertical flow pathways through the vadose zone, which would otherwise minimize the distance along which leachate could be 'cleaned' by aerobic processes en route to the water table, are offset by the long residence times.

During the study period, the rapid reduction in hydrological response (i.e. flux) with depth in the vadose zone accounted for the small and delayed storm-based response of the phreatic zone. Again, this indicates that water and effluent movement through the soil system was confined to the matrix pore-space, and that macropore flow was not a significant flow mechanism within this hillslope during the study period. Given the vadose zone flux and residence time calculations, the data suggest that water table recharge is derived from pre-event soil water stored within the lower C horizon. This water is mobilized during rainfall by steepened hydraulic gradients in the overlying horizons, and displaced towards the phreatic zone. These results may help explain some of the patterns observed by Heisig (2000) and shed further light on the amount of 'memory' there may be in hillslopes and watersheds impacted by septic systems.

#### ACKNOWLEDGEMENTS

The authors are grateful to Tom and Edie Keasbey for allowing us unrestricted access to their property during the course of the field experimentation. This research was conducted as part of the New York City Department of Environmental Protection Septic Siting Study (contract number 090065).

#### REFERENCES

- Amoozegar A. 1997. Comparison of saturated hydraulic conductivity and percolation rate: implications for designing septic systems. In *Site Characterization and Design of On-site Septic Systems*, Bedinger MS, Fleming JS, Johnson AI (eds). Special Technical Publication 1324, American Society for Testing and Materials (ASTM): Fredericksburg, Vancouver; 129–143.
- Anderson DL, Tyl MB, Otis RJ, Mayer TG, Sherman KM. 1998. Onsite wastewater nutrient reduction systems (OWNRS) for nutrient sensitive environments. In *On-Site Wastewater Treatment*, Sievers DM (ed.). Proceedings of the Eighth National Symposium on Individual and Small Community Sewage Systems, 8–10 March, Orlando, Florida. American Society of Agricultural Engineers: Michigan; 436–445.
- Brown KW, Wolf HW, Donnelly KC, Slowey JF. 1979. The movement of fecal coliforms and coliphages below septic lines. *Journal of Environmental Quality* **8**: 121–125.
- Buckingham E. 1907. *Studies on the Movement of Soil Moisture*. Bureau of Soils, US Department of Agriculture; Washington, DC; 38.
- Bureau of the Census. 1992. *1990 Census of Housing*. Department of Characteristics of Housing Units, Detailed Housing Characteristics, United States Summary, US Department of Commerce: Washington; 16.
- Canter LW, Knox RC. 1985. *Septic Tank System Effects on Ground Water Quality*. Lewis Publishers: Michigan.
- Cogger CG, Hajjar LM, Moe CL, Sobsey MD. 1988. Septic system performance on a coastal barrier island. *Journal of Environmental Quality* **17**: 401–408.
- Curry DS. 1999. *Final Report for the Septic Siting Project*. New York City Department of Environmental Protection Report.
- Darcy H. 1856. *Les fontaines publiques de la ville de Dijon*. Victor Dalmont: Paris.
- Harman J, Robertson WD, Zanini L. 1996. Impacts on a sand aquifer from an old septic system: nitrate and phosphate. *Groundwater* **34**: 1105–1114.

- Harr RD. 1977. Water flux in soil and subsoil on a steep forested slope. *Journal of Hydrology* **33**: 37–58.
- Heisig P. 2000. *Effects of Residential and Agricultural Land Uses on the Chemical Quality of Baseflow of Small Streams in the Croton Watershed, Southeastern New York*. Water-Resources Investigations Report 99-4173, U.S. Geological Survey: Reston, Virginia.
- Huang F. 1999. Development of an influent flow monitoring and autosampling system for onsite wastewater treatment systems. *The Small Flows Journal* **5**(1): 12–19.
- Lawrence CH. 1973. Septic tank performance. *Journal of Environmental Quality* **36**: 226–228.
- McKay LD, Balfour DJ, Cherry JA. 1998. Lateral chloride migration from a landfill in a fractured clay-rich glacial deposit. *Ground Water* **36**: 988–999.
- Millington RJ, Quirk JP. 1960. Permeability of porous solids. *Transactions of the Faraday Society* **57**: 1200–1207.
- Penninger PG, Hoover MT. 1998. Performance of an at-grade septic system preceded by a pressure-dosed filter on a wet, clayey belt soil. In *On-site Wastewater Treatment*, Sievers DM (ed.). Proceedings of the Eighth National Symposium on Individual and Small Community Sewage Systems, 8–10 March, Orlando, Florida. American Society of Agricultural Engineers: Michigan; 326–335.
- Rawls WJ, Brakensiek DL. 1989. Estimation of soil water retention and hydraulic properties. In *Unsaturated Flow in Hydrologic Modelling Theory and Practice*, Morel-Seytoux HJ (ed.) NATO ASI Series. Series C. Mathematical and Physical Science, Vol. 275. Kluwer Academic: Dordrecht; 275–300.
- Robertson WD, Cherry JA, Sudicky EA. 1991. Ground-water contamination from two small septic systems on sand aquifers. *Ground Water* **29**: 82–92.
- Sherlock MD, Chappell NA, McDonnell JJ. 2000. Effects of experimental uncertainty on the calculation of hillslope flow paths. *Hydrological Processes* **14**: 2457–2471.
- Van Genuchten Mth. 1980. A closed-form equation for predicting the hydraulic conductivity of unsaturated soils. *Soil Science Society of America Journal* **44**: 892–898.
- Wernick BG, Cook KE, Schreier H. 1998. Land use and streamwater nitrate-N dynamics in an urban-rural fringe watershed. *Journal of the American Water Resources Association* **34**: 639–650.
- Wilhelm S, Schiff S, Robinson W. 1996. Biogeochemical evolution of domestic waste water in septic systems: 2. Application of a conceptual model in sandy aquifers. *Groundwater* **34**: 853–864.
- Wilson GV, Alfonsi JM, Jardine PM. 1989. Spatial variability of saturated hydraulic conductivity of the subsoil of two forested watersheds. *Soil Science Society of America Journal* **53**: 679–685.
- Wolf DC, Gross MA, Earlywine KE, Davis KJ, Rutledge EM. 1998. Renovation of onsite domestic wastewater in a poorly drained soil. In *On-site Wastewater Treatment*, Sievers DM (ed.). Proceedings of the Eighth National Symposium on Individual and Small Community Sewage Systems, 8–10 March, Orlando, Florida. American Society of Agricultural Engineers: Michigan; 320–325.